The Protein Journal (2022) 41:260–273
https://doi.org/10.1007/s10930-022-10044-x

A Phagosomally Expressed Gene, *rv0428c*, of *Mycobacterium tuberculosis* Demonstrates Acetyl Transferase Activity and Plays a Protective Role Under Stress Conditions

Aashish Sharma[1,2] · Arbind Kumar[1,2] · Mudasir Rashid[3] · Ramchandra Vijay Amnekar[4] · Sanjay Gupta[3] · Jagdeep Kaur[1]

Accepted: 31 January 2022 / Published online: 17 February 2022

Abstract

Mycobacterium tuberculosis genome is composed of several hypothetical gene products that need to be characterized for understanding the physiology of bacteria. Rv0428c was one of the 11 proteins exclusively identified within the phagosomal compartment of macrophages infected with mycobacteria and marked as hypothetical. The expression of *rv0428c* gene was upregulated under acidic and nutritive stress conditions in *M. tuberculosis* H37Ra, which was supported by potential sigma factor binding sites in the region upstream to the *rv0428c* gene. The bioinformatics analysis predicted it to be a GCN5- acetyl transferase, belonging to the Histone acetyl transferase (HAT) family. The docking analysis predicted formation of hydrogen bonds and hydrophobic interactions between donor acetyl-co-A and histone H3 tail region. *rv0428c* gene was cloned and expressed in *E. coli.* The protein was purified to homogeneity and was fairly stable over a wide range of pH 5.0–9.0 and temperature up to 40 °C. The HAT activity of purified Rv0428c was confirmed by in vitro acetylation assay using recombinant H3 histone expressed in bacteria as substrate, which increased in time dependent manner. The results suggested that it is the second confirmed acetyl transferase in *M. tuberculosis* H37Rv. Furthermore, *rv0428c* was over expressed in surrogate host *M. smegmatis*, which led to enhanced growth rate and altered colony morphology. The expression of *rv0428c* in *M. smegmatis* promoted the survival of bacteria under acidic and nutritive stress conditions. In conclusion, Rv0428c, a phagosomal acetyl transferase of *M. tuberculosis,* might be involved in survival under stress conditions.

Keywords *Mycobacterium tuberculosis* · Histone acetyl transferase (HAT) · Stress · Chloramphenicol

1 Introduction

Tuberculosis (TB) is amongst the most infectious diseases that has inflicted mankind. Every third individual is infected with *Mycobacterium tuberculosis*. According to WHO, an estimated 1.4 million deaths were reported from tuberculosis worldwide with nearly 0.2 million individuals being Human Immunodeficiency Virus (HIV)-positive [1]. There has been no respite from the woes of *M. tuberculosis* due to its poorly understood biology, survival strategies, life cycle and pathogenesis [2, 3]. The genome of *M. tuberculosis* was sequenced way back in 1998, identifying approximately 4000 proteins with 40% of these annotated as hypothetical proteins [4]. For better understanding of the physiology and virulence of this bacterium, there is an urgent need for assigning specific roles to these hypothetical proteins by detailed characterization.

M. tuberculosis is an intracellular pathogen with a dynamic proteome, which plays a role in survival of the pathogen under stress conditions encountered within the host macrophages [5]. The immense success of this bacterium as a pathogen is dependent upon it's capability to utilize the host macrophages for survival and proliferation by

✉ Jagdeep Kaur
jagsekhon@yahoo.com; jagsekhon@pu.ac.in

[1] Department of Biotechnology, Panjab University, BMS Block-1, South Campus, Chandigarh 160014, India

[2] Present Address: COVID-19 Testing Facility, CSIR-IHBT, Palampur 176061, India

[3] Epigenetics and Chromatin Biology Group, Gupta Lab, Cancer Research Institute, Advanced Centre for Treatment, Research and Education in Cancer, Tata Memorial Centre, Kharghar, Navi Mumbai, MH 410210, India

[4] Homi Bhabha National Institute, Training School Complex, Anushakti Nagar, Mumbai, MH, India

employing various strategies [6]. These include prevention of the lysosome phagosome fusion and acidification of the phagosome, protection from reactive oxygen radicals and altering the immune response [7]. Intraphagosomal microbes were reported to alter host cell physiology. In some cases it can induce apoptosis, while macrophages containing mycobacterium in phagosomes are known for long term survival. For its intraphagosomal survival, mycobacterium has to deal with various intracellular stress conditions such as hypoxia, acidic, oxidative, nutritive and iron stress [8].

The 2-dimesional gel electrophoresis and Mass spectrometry analysis of intraphagosomally grown mycobacteria in bone marrow macrophages, identified 11 exclusively present mycobacterial proteins [9]. These proteins needed special attention to pin point their role in intracelluar survival of *M. tuberculosis.* Six of the total 11 identified phagosomal mycobacterial proteins, i.e., Rv2691, Rv1627c, Rv1191, Rv1130, Rv0489 and Rv0428c, were unique as these were not noticed in in vitro growth of mycobacterium. Out of the above mentioned six proteins, Rv1191, Rv1130 and Rv0428c were reported as conserved hypothetical proteins. As Rv0428c has not been characterized yet, it was selected for detail characterization.

The bioinformatics analysis predicted Rv0428c to be a GCN5- acetyl transferase belonging to the Histone acetyl transferase family (HAT). HAT proteins are involved in acetylation of core histones, which further results in important regulatory effects on chromatin structure, assembly and gene transcription. Till date only one mycobacterium protein, eis (enhanced intracellular protein), has been shown to possess N^{ε}-acetyltransferase activity [10].

Rv0428c was reported to be specifically present in pathogenic strains like *M. tuberculosis*, *M. bovis* and clinical strain *CDC1551,* but is conspicuously absent in non-pathogenic *M. smegmatis* strain pointing towards some critical role played by this gene in pathogenesis/virulence. In the present investigation, attempt has been made to characterize Rv0428c by biochemical and biophysical methods. The expression of Rv0428c was studied under normal and stress conditions. The effect of expression of *rv0428c* on colony morphology and growth pattern was monitored in surrogate host *M. smegmatis* which lacks *rv0428c* gene sequence in its genome. The experiments were also carried out to investigate the role of Rv0428c in conferring drug resistance.

2 Material and Methods

2.1 Bacterial Strains and Plasmids

The bacterial strains used in the study were procured from IMTECH, Chandigarh. The strains which were used included *E. coli* DH5α, *E. coli* BL21 (DE3) and *M. tuberculosis* H37Ra. The *E. coli* was grown in 2% Luria–Bertani (LB) broth and *Mycobacterium* H37Ra was cultured in 0.5% Middlebrook 7H9 (7H9) media supplemented with 1% glycerol and 0.05% Tween-80.

2.2 Expression of *rv0428c* in *M. tuberculosis* H37Ra Under Stress Conditions

M. tuberculosis H37Ra was grown in Middlebrook 7H9 media supplemented with 1% glycerol, 0.2% Tween-80 and 1% OADC. The culture was grown to mid-log phase (OD_{600} = 0.7–0.8) for 7 days and harvested by centrifugation. For exposure to various stress conditions, the bacterial pellet was re-suspended in appropriate media such as 7H9 growth media with 5 mM H_2O_2 for oxidative stress, 7H9 growth media at pH 4.5 for acidic stress, 1X PBS for nutrient stress and iron deficient media for iron stress. For acidic stress, the bacterial pellet was re-suspended in 7H9 liquid medium (pH 4.5) supplemented with 1% glycerol, 0.2% Tween 80 and 1% OADC and kept at 37 °C without shaking. Cells were harvested at 6 h. The culture grown in 7H9 medium at pH 7.2 served as a control for relative expression analysis. For oxidative stress administration, the bacterial pellet was re-suspended in 7H9 media containing 1% glycerol, 0.2% Tween 80, 1% OADC and 5 mM H_2O_2. The culture was then kept at 37 °C without shaking. The culture without H_2O_2 served as a control. Both the cultures were harvested after 6 h. RNA was isolated from the bacterial cultures and used for relative expression analysis. To administer nutritive stress, cells were washed twice with PBS containing Tween 80 (0.2%, v/v), pH 7.2 and then, re-suspended in 50 ml PBS containing Tween 20 (0.2%, v/v), (pH 7.2). Culture was incubated at 37 °C without shaking for 6 h. Three washings were given to the cells with PBS (pH 7.2) for removal of traces of media. Re-suspension of washed cells was done in iron deficient media. Supplementation of the control culture was done by adding 160 µM of $FeCl_3$. The cells were grown for 96 h and harvested for RNA isolation. Total RNA isolation was carried out for from all the samples using TRIzol method. Equal amount of RNA was used for cDNA preparation by using RevertAid™ first strand cDNA synthesis kit (Fermentas, USA). The expression analysis and quantification was done by using qRT-PCR (Applied Biosystems® StepOne TM Real-Time PCR Systems). The normalization of cDNA amount was done by using *sigA* as a reference gene.

2.3 Promoter Analysis

The promoter analysis of *rv0428c* gene was done by analyzing the 250 bp nucleotide sequence upstream to the operonic arrangement of the rv0428c. The sigma factor binding sites were identified and marked within this upstream DNA sequence.

2.4 In Silico Analysis

Multiple sequence alignment was performed by Clustal Ω, to study the extent of conservation and variation in protein sequences [11]. Espript 3 was used to assign the secondary structure to the alignment file [12]. The genomic organization of *rv0428c* gene of *M. tuberculosis* and its orthologs in *M. bovis* and *M. leprae* was checked by analyzing the gene sequences upstream and downstream to these genes in their respective genomes. The protein–protein interaction of Rv0428c protein was done by using STRING (Search Tool for the Retrieval of Interacting Genes/Proteins) database which predicts the possible interaction of the protein with other proteins that uses numerous sources, including experimental data, computational prediction methods and public text collections [13].

2.5 Homology Modelling

The blast protein hits showed BLASTP analysis of Rv0428c protein was performed against PDB proteins for selection of appropriate templates for generation of 3D structure models. The blast protein hits demonstrated that the identity and query coverage were found to be below 35%. Therefore, ab-initio based approach was utilised for protein modelling using I-TASSER program. Visualization of the 3D model structure of protein was done by using PyMol software [14, 15].

2.6 Binding Cavity Prediction

The analysis of binding pocket of Mtb Rv0428c was carried out by Computed Atlas of Surface Topography of proteins (CASTp) server [16]. This server was endowed with weighted Delaunay triangulation and the alpha complex framework which were used for measuring the shapes of molecules. It unveils inaccessible cavities and solvent accessible surface geometry in protein. The structural pockets and cavities were calculated in relation to area and volume by two approaches; solvent accessibl surface model (Richards' surface) and molecular surface model (Connolly's surface).

2.7 Grid Generation for Docking Studies

The ligand binding site of Rv0428c protein was predicted using COACH program [17]. As predicted, Gly183, Gly186, Ser215, Met137, Ala181, Arg187, Trp190, Thr212 and Val216 from Rv0428c were involved in binding with acetyl-co-A, whereas, Gly128, Val151, Trp122, Leu125, Ala152 and Arg155 of Rv0428c were found to be involved in binding with histone H3 tail region. A grid was generated in the region of these predicted binding site residues of prepared protein by means of the Autodock tools [18]. For docking procedures, Autodock Vina was used at its default parameters. Through Autodock tools, protein and ligands were generated in pdbqt formats. The gasteiger charge and polar hydrogen were assigned to the receptor and ligands. The grid boxes were set in the range of approximately $30 \times 30 \times 30$ point size, spaced at 0.375 Å in each direction around the cavity for accommodating the ligands.

2.8 Cloning, Expression and Purification of Rv0428c

M. tuberculosis H37Rv chromosomal DNA was a kind gift from Dr. U. D. Gupta, JALMA, Agra. The 18 to 24 bases were selected from the terminal region of gene sequences and analysed by integrated oligoanalyzer tools for optimal designing of primers (Integrated DNA Technologies, Inc., U.S.A., http://eu.idtdna.com/ site). Optimization of Tm, GC content and hairpin loop structure of primers was carried out [19]. The primers used in the study are specified in Table 1. For cloning of *rv0428c*, gene sequence was amplified by designated set of primers by using genomic DNA of *M. tuberculosis* H37Rv as a template. Amplified *rv0428c* and circularized expression vector pET28a were digested with *BamHI/HindIII* restriction enzymes. The excised gene of interest and digested lineralized pET28a vector were purified from the gel and ligation reaction was set up. The ligated product was transformed into *E. coli* DH5α ultra competent cells. The recombinant clones were confirmed by sequencing (Chromous Biotech, India). The positive recombinant clone was further used to transform expression host *E. coli* BL21 (DE3). *E. coli* BL21 (DE3) cells harbouring *rv0428c* were induced with 0.06 mM isopropyl–D-thiogalactopyranoside (IPTG) and grown at 18 °C, 180 rpm for 16 h [20, 21]. The recombinant protein was expressed in

Table 1 Primers used in the course of study

Gene	Primer pairs	Annealing (°C)
rv0428c (pET28a)	FWD-5′AAGGATCCATGGTCTCGTGGCCTGGACTT 3′ REV-5′ ACAAGCTTCTCGAAGGTATCCCAGCCGAC 3′	60
rv0428c (pvv16)	FWD-5′AAGGATCCATGGTCTCGTGGCCTGGACTT 3′ REV-5′ AAGGATCCATAGAAGGTATCCCAGCCGACC 3′	60
rv0428c (Stress)	FWD-5′CACCATCACAGAAATCAGCGC 3′ REV-5′GGTGGTCCAGCAACGTGA 3′	53

soluble fraction and was purified to homogeneity by Nickel-nitrilotriacetic acid (Ni–NTA) chromatography. The integrity and purity of protein was analyzed on 12% SDS-PAGE.

2.9 Biophysical Characterization of rRv0428c

Biophysical characterization was carried out by performing CD spectroscopy and fluorescent spectroscopy. CD spectroscopy analysis was carried out by measuring Far UV-CD spectra of rRv0428c protein with a JASCO J-815 spectrofluorometer. Far UV-CD spectra were collected over the wavelength range of 195–250 nm at 25 °C. To study the effect of temperature, 200 µg of protein was incubated at temperatures ranging from 30 to 70 °C for 30 min. The spectra were collected over a range of 200–240 nm wavelengths with a band width of 1 nm and response time of two seconds. The CD values were expressed as molar ellipticity ([θ], $degcm^2\ dmol^{-1}$). For studying the effect of pH, 200 µg protein was incubated with 50 mM phosphate buffer of varying pH from 5.0 to 11.0 for 30 min and the spectra were collected from 200 to 240 nm wavelengths. The fluorescence spectrum of rRv0428c protein was measured using JASCO J-815 spectrofluorometer using a 10 mm path length quartz cuvette. For determining the intrinsic tryptophan fluorescence, the excitation wavelength used was 295 nm with emission measured in the range of 310–400 nm. The spectra were recorded from 20 to 90 °C by incubating the protein for 30 min.

2.10 Biochemical Characterization of rRv0428c

In vitro acetylation assay for rRv0428c was performed by using bacterially expressed recombinant histone H3 as substrate and acetyl-coA as a donor molecule and mammalian core histones as a positive control. The reaction was set up in acetyl-transferase assay buffer (50 mM Tris–Cl, pH 8, 10% glycerol, 10 mM butyric acid, 0.1 mM EDTA, 1 mM DTT, 1 mM PMSF) with 10 µM acetyl-coA, 10 µg histone H3, with rRv0428c. A time dependent kinetics was studied by incubating the reaction mixture for 1 h, 2 h and 3 h, in a 30 °C water bath followed by addition of 2X SDS-PAGE sample buffers and 10 min boiling for stopping the reaction. The prepared samples were then subjected to 18% SDS-PAGE gel electrophoresis and transferred onto PVDF membranes. The membrane was stained with 0.05% Fast green for validating equal loading of samples followed by western blotting with Anti H3K9ac antibody (1:5000, Millipore).

2.11 Cloning and Growth Pattern Analysis of *rv0428c* Gene in *M. smegmatis* Using *E. coli—Mycobacterium* Shuttle Vector

rv0428c was amplified from the recombinant pET28a plasmid using primers mentioned in Table 1. Amplified gene product was separated on a 1.2% agarose gel and the fragments were subsequently excised and eluted. Amplified *rv0428c* and *pVV16* plasmid were digested with *BamHI* restriction enzyme followed by purification of cut fragments. The digested products were ligated using T4 DNA ligase. *M. smegmatis* mc^2155 was grown in 7H9 broth supplemented with 1% glycerol, 1% OADC and 0.2% Tween 80 at 37 °C, 180 rpm till the OD_{600} reached 0.6–0.8. The cells were harvested by centrifugation at 4000 rpm at 4 °C. Cells were incubated on ice for 2 h. Then, cells were washed three times with 10% glycerol by centrifugation at 4000 rpm for 10 min. Cells were re-suspended in 10% glycerol at 1/500th of original volume. The recombinant plasmid and *pVV16* alone (5 ng) were added to the 100 µl electrocompetent *M. smegmatis* mc^2155 cells and transferred to 0.2 cm Biorad electroporator cuvette. The cells were then incubated on ice for 10 min. The electroporation was carried out at 25 µF and 2.5 kV for 5 ms using Gene pulser, BioRad, USA followed by addition of 7H9 media immediately. The electroporated cells were then incubated at 37 °C, 180 rpm for 6 h. Finally, the cells were spread onto 7H10 agar plates containing Kan^+.

M. smegmatis harbouring *pVV16-rv0428c* or *pVV16* alone were inoculated in 10 ml M7H9 media supplemented with 0.1% glycerol, 0.2% Tween 80 and 1% OADC at 180 rpm, 37 °C. Next day, the cultures were sub-cultured in 100 ml flask containing M7H9 media supplemented with 0.1% glycerol, 0.05% Tween 80 and 1% OADC after normalization of A_{600}. The cultures were further grown at 37 °C and 180 rpm. The growth pattern was measured by taking absorbance at 600 nm and CFU counting at regular time intervals. To study the differences in colony morphology of *M. smegmatis* harbouring *pVV16-rv0428c* or *pVV16* alone, both the strains were plated onto M7H10 plates supplemented with 0.1% glycerol, 0.2% Tween 80 and 1% OADC and incubated at 37 °C for 5–6 days. Microphotography of the colonies was carried out.

2.12 Survival of *Msmeg-rv0428c* Under Stress Conditions In Vitro

2.12.1 Acidic Stress

The cultures *Msmeg-pVV16-rv0428c* (test) and *Msmeg-pVV16* (control) were grown in M7H9 liquid media as described previously in 10 ml tubes. Next day, sub-culturing of both the cultures was carried out in 20 ml M7H9 media (pH 7.2), M7H9 media (pH 6.0) and M7H9 media (pH 5.0) flasks containing 1% OADC to make the final absorbance 0.5 at 600 nm. The survival was checked by plating suitable dilutions of the cultures onto M7H10 agar plates having kanamycin at 37 °C for 2–3 days.

2.12.2 Nutritive Stress

For induction of nutritive stress conditions, both the cultures *Msmeg-pVV16-rv0428c* (test) and *Msmeg-pVV16* (control) were grown overnight in 10 ml M7H9 tubes at 180 rpm at 37 °C. Further sub-culturing was carried out in 20 ml flasks containing 1X PBS. The final absorbance was normalized to 0.5 at 600 nm. The cultures were then incubated at 180 rpm at 37 °C for 12 h and 24 h followed by spreading of appropriate dilutions onto M7H10 plates containing kanamycin and incubating the plates for 2–3 days at 37 °C.

2.12.3 Oxidative Stress

For oxidative stress administration, the bacterial pellet was re-suspended in M7H9 media containing 1% glycerol, 0.2% Tween 80, 1% OADC and 5 mM H_2O_2. The culture was then kept at 37 °C without shaking. The culture without H_2O_2 served as control. Both the cultures were harvested after 6 h. RNA was isolated from the bacterial cultures and used for relative expression analysis.

2.12.4 Iron Stress

Cells were washed thrice with PBS (pH 7.2) followed by two washings with iron deficient media to remove any traces of culture media. The washed cells were further re-suspended in iron deficient media. The control culture was supplemented with 160 µM of $FeCl_3$. The cells were grown for 96 h and harvested for RNA isolation.

2.13 Drug Susceptibility Testing (DST)

Resazurin redox indicator test was used for checking the effect of Rv0428c protein on drug susceptibility (Palomino et al., 2002). The susceptibility of *Msmeg-rv0428c* and *Msmeg-pVV16* was determined against various drugs- streptomycin, chloramphenicol, isoniazid and rifampicin. The bacterial cultures were grown to mid-log phase and diluted for equal dispensation of the cells (4×10^5) in 48-well plates. The reason for using mid-log phase bacterial cells was that these exhibit constant growth rate and have an optimal level of expression. The drugs were diluted to working concentration ranges in M7H9 media without the detergent Tween-80. Different concentrations of drugs was added and incubated at 37 °C for 2 h. A working 1:1 dilution of 10X stock resazurin was prepared in 20% tween-80 and 8 µl of it was added per well in 48-well plates. The viable bacteria lead to conversion of resazurin to resurfin which was monitored by the change in colour of the medium from blue to pink. The survival of *Msmeg-pVV16-rv0428c* and *Msmeg-pVV16* was also monitored by counting the CFU/mL after treatment with chloramphenicol.

3 Results

3.1 Upregulation of *rv0428c* in Acidic and Nutritive Stress Conditions

rv0428c protein was detected exclusively in the phagosomal compartment of macrophages infected with *M. tuberculosis*, making it an ideal candidate for being involved in playing a regulatory role during stress encounter. We, thereby, proceeded for analyzing the expression of *rv0428c* in various stress conditions including acidic, oxidative, nutritive and iron stress *in-vitro* in *M. tuberculosis* H37Ra. Semi quantitative PCR analysis demonstrated upregulation of *rv0428c* in acidic and nutritive stress by 5.4 and 3.6 fold, respectively (Fig. 1A, B). The analysis of upstream regulatory promoter region showed the presence of two putative sigma factors binding sites i.e. s*igE* (CGACAT(15-19)GGTTC) and *sigF* (GGCGAA(16-20) SGTTS), which were previously implicated in acidic and nutritive stress conditions [22, 23] (Fig. 1C).

3.2 In Silico Analysis of Rv0428c

The gene *rv0428c* and protein sequence was retrieved from TubercuList database. The size of the gene is 909 bp and it encodes a protein of 302 amino acids. It is predicted to be involved in intermediary metabolism and contains GNAT domain at C- terminal [24]. Rv0428c has orthologs in three other pathogenic mycobacterium species *M. bovis, M. leprae* and *M. canettii*. GCN5-related N-acetyltransferase from *Kribbella flavida* with PDB_ID 4IUS showed maximum identity with Rv0428c protein and was used as a template for performing multiple sequence alignment. Multiple sequence alignment revealed the conserved regions between the Rv0428c protein and its counterparts in other Mycobacterium species (Sup Fig. 1). In prokaryotes, the genomic organization of a gene is often considered in speculating on the probable gene function based on its positional counterpart or gene organization. The gene encoding for Rv0428c in *M. tuberculosis* is flanked by probable polypeptide deformylase (*def*) and exodeoxyribonuclease III (*xthA*) in the genomic organization. This genomic organization is also conserved in *M. bovis* and *M. leprae* (Fig. 2A). The Rv0428c protein possessed the VAPTHRRRG sequence similar to the V/I-X-X-X-X-Q/R-X-X-G consensus sequence of GCN5-acetyl transferases suggesting that Rv0428c is a probable member of the GCN5-acetyl transferase family. The interaction studies revealed that Rv0428c protein interacted with several proteins including the eis (enhanced intracellular survival) protein of *M. tuberculosis* which is an N^{ε}-acetyl transferase (Sup Fig. 1).

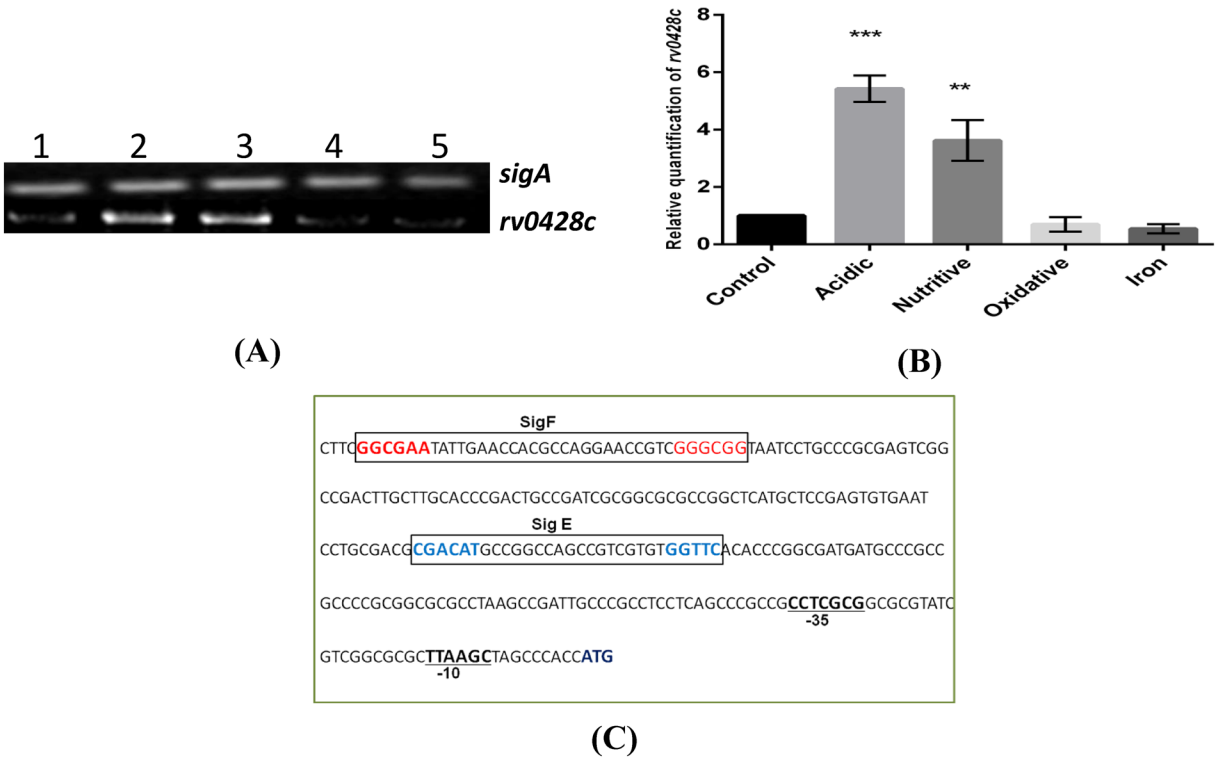

Fig. 1 Expression analysis of *rv0428c* under different *in-vitro* stress conditions by real- time PCR. **A** RT-PCR analysis, Amplification of *Sig A* gene as internal control and *rv0428c* gene from prepared cDNAs under different stress conditions. *L1* control, *L2* acidic, *L3* nutritive, *L4* Oxidative, *L5* iron **B** qPCR analysis of *rv0428c* expression under various *in-vitro* stress conditions **C** Diagrammatic representation of putative binding sites in the promoter region of *rv0428c* gene, *sigF* binding site is highlighted in red color in a box, *sigE* binding site is highlighted in blue color. Given values are expressed in mean ± *SD* performed in three independent experiments. Statistical analysis was assessed using student's *t*-test (*$p \leq 0.05$, **$p \leq 0.01$ and ***$p \leq 0.001$)

3.3 3D Model Structure of Rv0428c Protein and Structural Alignment

The model of Rv0428c protein was generated by using I-TASSER. A set of 5 models were constructed based on the 10 best templates. The models generated were sorted based on their C-scores, which represent the confidence in the predicted structure on the basis of threading template alignments and convergence parameters involved in the simulation [17]. The range for C-score lied between − 5 and 2 with higher C-score signifying a model with higher confidence. The C-score for Rv0428c model lied in the permissible range and was found to be − 0.40. Depending upon the C-score, TM-score and RMSD values were calculated. The model had a TM-score of 0.66 ± 0.13 and RMSD value of 6.6 ± 4.0 Å. The final PROCHECK program measured the Ramchandran plot statistics, which showed that around 80% of the residues are in the most favoured region. Quality of the generated models was assessed by Verify 3D and QMEAN score 4. Verfy3D result demonstrated that the 80% of the amino acids are in the acceptable range (≥ 0.2 in the 3D/1D profile). QMEAN score is below 0.5 which showed the accuracy of predicted model for further experimental use (Supp. Figure 2). These statistics confirmed that our predicted model had precise topology. The alignment analysis of Rv0428c protein with the template GCN5-related N-acetyltransferase from *Kribbella flavida* (PDB_ID: 4IUS) was done (Fig. 2B). The superimposition of 3D models of Rv0428c protein and template GCN5-related N-acetyltransferase from *Kribbella flavida* (PDB_ID: 4IUS) revealed overlapping of the α-helices and β-strands (Fig. 2C).

3.4 Cavity Prediction and Analysis

Acetyl coenzyme-A (AcoA) acted as a donor of acetyl group for conversion of conserved lysine amino acid residues on histone proteins to be acetylated to ε-N-acetyl lysine and hence regulating the gene expression. As Rv0428c is a probable GCN5-acetyl transferase, we docked the acetyl-co-A molecule in the binding pocket of Rv0428c protein. The size of the cavity of Rv042c protein was predicted by using CASTp algorithm. Histone H3 was used as substrate because most of the histone acetylation events take place on H3, for interacting with the cavity as the substrate for GCN5-acetyl

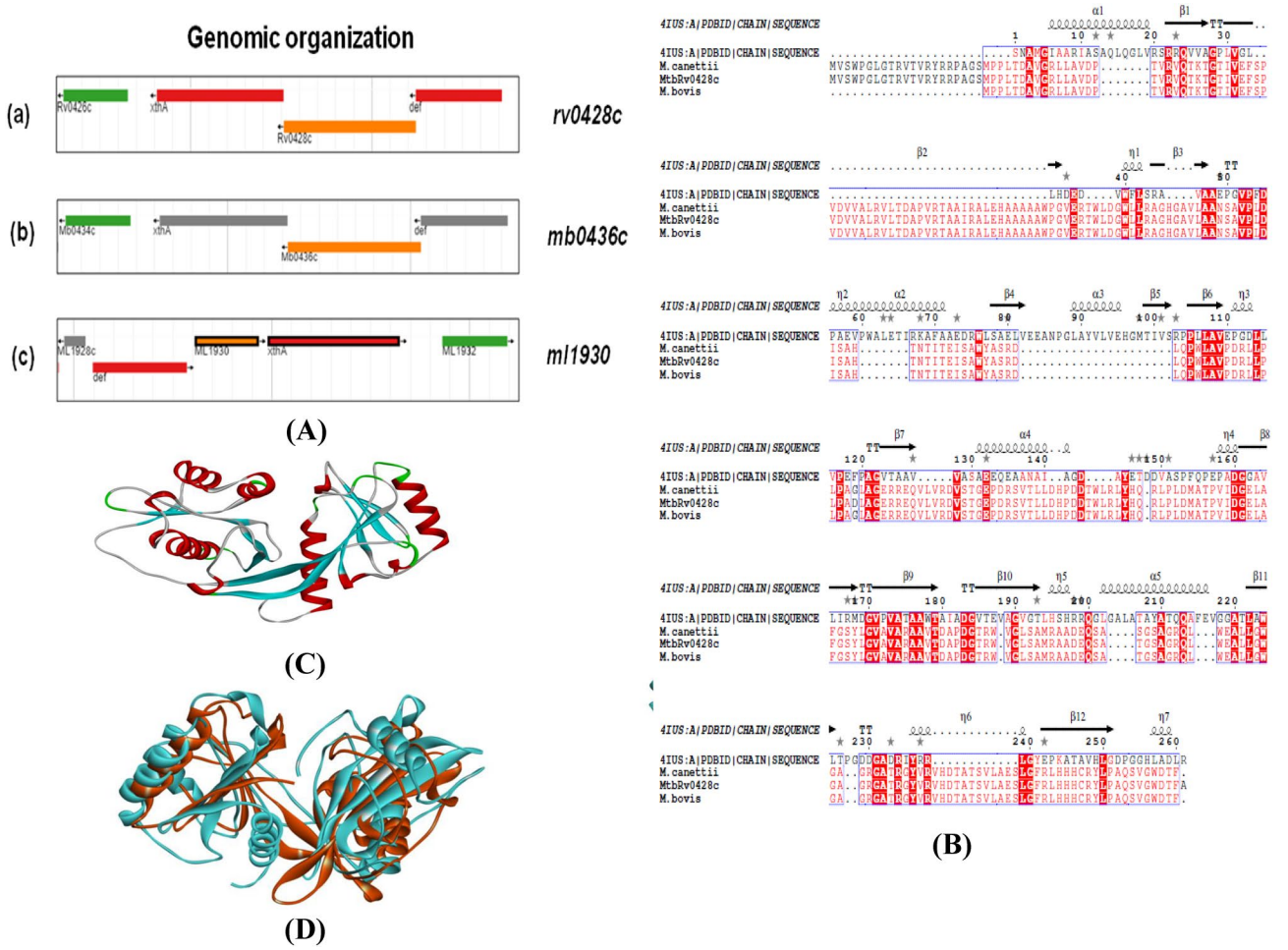

Fig. 2 **A** Map showing the genomic organization of *rv0428c* in *M. tuberculosis* H37Rv and its counterparts *mb0436c and ml1930 in M. bovis* and *M. leprae* **B** Multiple sequence alignment of Rv0428c protein sequence with its orthologs was obtained with the Clustal Ω program and conserved regions were assigned to the aligned file by Espript 3.0. Red Shading indicates residues identical in all the protein sequences **C** Molecular 3D model of Rv0428c: The helices were represented in red, β-sheets in cyan and random coils in green. Image was generated through Discovery studio 4 **D** The superposition of the structure of bacterial GCN5-related N-acetyltransferase from *Kribella flavida* and the 3-D structure model of the Rv0428c protein**.** PDB_ID: 4IUS is represented in maroon and Rv0428c in cyan

transferase is histone H3. The binding pocket size for acetyl-co-A and histone H3 tail were calculated. The binding pocket volume for acetyl-co-A was observed to be 30.9 Å and area was 94.6 Å, whereas, in case of histone H3 tail region, the volume was 34.9 Å with an area of 88.6 Å (Table 2). The binding energy was found to be − 6.1 and − 5.8 kcal/mol for acetyl-co-A and histone H3 tail, respectively.

Table 2 Binding pocket size of Rv0428c protein

Protein	Ligand	Binding pocket volume (Å)	Binding pocket area (Å)
Rv0428c	Acetyl-co-A	30.9	94.6
	H3 tail	34.9	88.6

3.5 Docked Acetyl-co-A and Histone H3 Tail with the Binding Pocket of Rv0428c Protein

Acetyl-co-A has a molecular weight of 809.57 g/mol. The complex of Rv0428c-acetyl-co-A was stabilized by the formation of hydrogen bonds and hydrophobic interactions. The acetyl-co-A was docked against Rv0428c protein (Fig. 3A). The H-bonds were formed between Gly185, Asp223 and Gly224 amino acid residues of Rv0428c and acetyl-co-A. The distances between the donor and acceptor molecules was computed on the basis of maximum acceptor (A) and H-bond donor (D) and were found to be 3.07 Å, 2.92 Å and 3.02 Å, respectively. Several hydrophobic interactions were also observed which included Met137, Ala181, Arg192, Asp223, Ala225 and Thr272 (Fig. 3B).

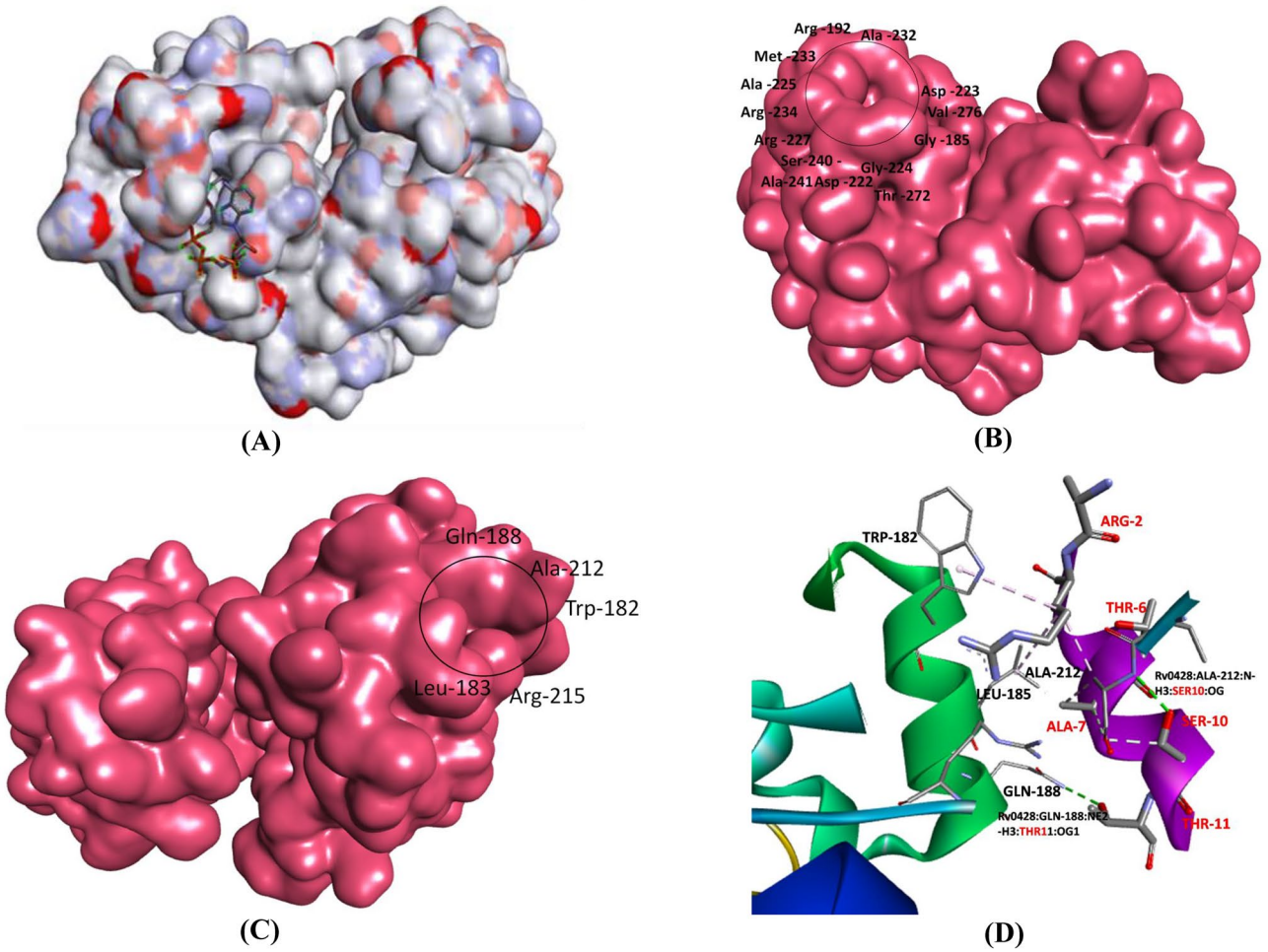

Fig. 3 Docking analysis of Rv0428c protein **A** Docking of acetyl-co-A in the binding pocket of Rv0428c protein. **B** Cavity residues of Rv0428c protein involved in interaction with acetyl-co-A **C** Cavity residues of Rv0428c protein involved in interaction with histone H3 tail region. **D** Zoomed in view of interaction between histone H3 tail and Rv0428c protein, The green coloured helical structure represents Rv0428c protein and red colour corresponds to histone H3 tail

The histone H3 tail was 14 amino acids long with molecular weight of 1.45 kDa. The formation of hydrogen bonds and hydrophobic interactions stabilized the protein–protein interactions between Rv0428c protein and H3 tail region. The H-bonds were formed between Leu183 and Gln188 amino acids of Rv0428c protein and H3 tail. The distance between the donor and acceptor were found to be 2.99 Å and 2.96 Å, respectively. The hydrophobic interactions between Trp182, Ala212, and Arg215 were observed (Fig. 3C, D; Table 3). The docking of acetyl-co-A and H3 tail results signified that these molecules interact with our protein of interest, Rv0428c and might help in acetylation of histone proteins further leading to regulation of gene expression.

3.6 Cloning, Expression and Purification of *rv0428c*

For expression and purification studies, pET^{Rv0428c} plasmid was transformed in *E. coli* BL21 DE3 cells. Rv0428c protein was expressed in soluble fraction and was purified by Ni–NTA chromatography to homogeneity as demonstrated by a single band on SDS-PAGE with an approximate molecular mass of 35 kDa (Fig. 4A).

Table 3 Residues involved in complex stability through hydrogen and hydrophobic interactions

Protein	Compound	H-bond donor	H-bond acceptor	Distance (Å)	Hydrophobic bonds
Rv0428c	Acetyl-co-A	Gly185 (N) Asp223 (OD) Gly224 (N)	AcoA (O9) AcoA (O9) AcoA (O2)	3.07 2.92 3.02	Arg192, Thr272, Asp223, Ala225
	H3 tail	Gln188 (NE2) Leu183 (N)	H3 (OG1) H3 (CG)	2.99 2.96	Trp182, Ala212, Arg215

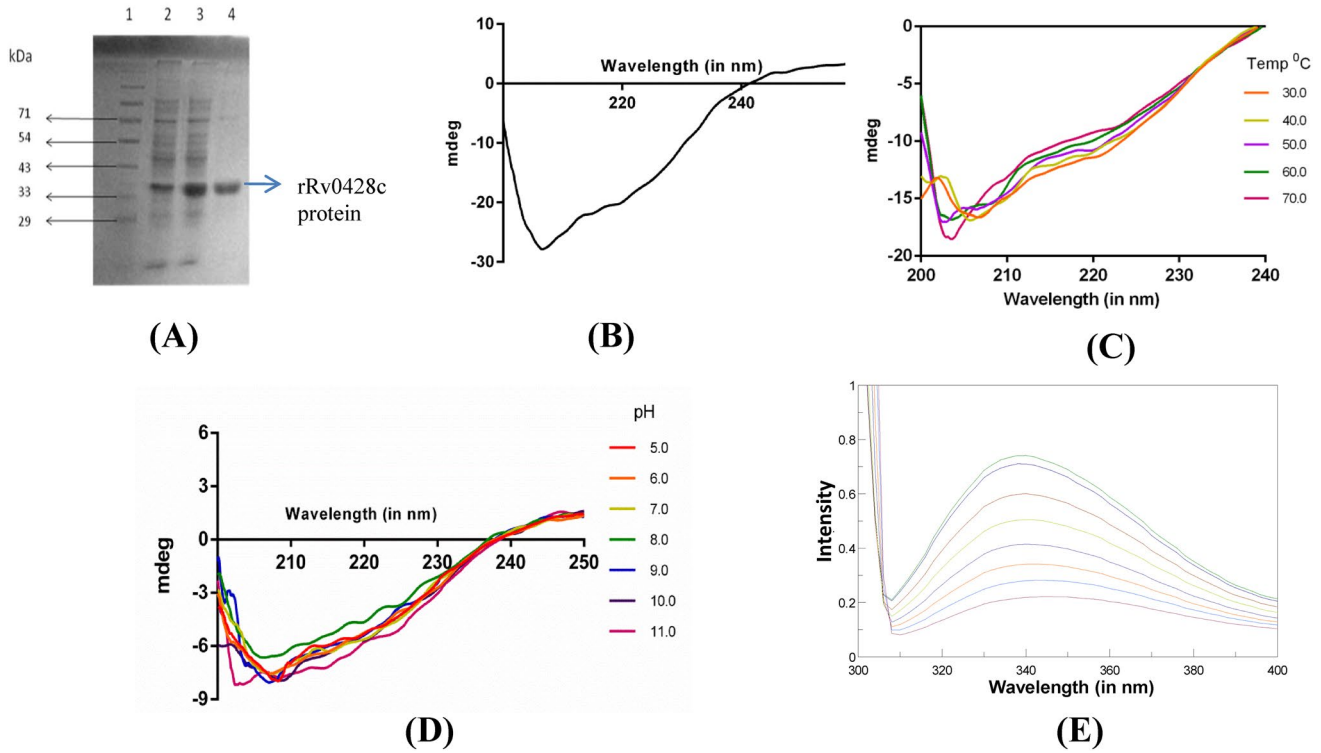

Fig. 4 **A** Expression analysis of recombinant Rv0428c protein on 10% SDS PAGE *L1* Protein marker, *L2* Pellet of uninduced rRv0428c culture, *L3* Pellet of culture induced with 60 µm IPTG at 18 °C and *L4* Purified rRv0428c protein **B** Far–UV CD spectra of recombinant purified rRv0428c protein measured in 10 mM phosphate buffer (pH 8.0) at 25 °C at wavelength 190–260 nm **C** Far UV CD spectra recorded at temperatures ranging from 30–70 °C demonstrated gradual decrease in the negative ellipticity with subsequent increase of temperature **D** Far UV CD spectra of rRV0428c protein after incubating the protein for 1 h with different buffers of pH- 5.0–9.0 demonstrated that Rv0428c protein was stable over a wide range of pH **E** Fluorescence spectra of purified rRv0428c protein at different temperatures (20 to 90 °C) recorded from 310 to 400 nm wavelength demonstrated gradual decrease in the intrinsic fluorescence with the subsequent increase in temperature

3.7 Biophysical Characterization of rRv0428c Protein

3.7.1 Secondary Structure Content of rRv0428c Protein

Far UV CD spectrum (190–260 nm) of rRv0428c protein was recorded using the J-815 CD spectropolarimeter at room temperature. The spectrum revealed the characteristic negative ellipticity comprising of both α- helix and β- sheets in the secondary structure (Fig. 4B). The secondary structure of protein was determined by spectra analysis software. Relative amount of structural element estimated for the rRv0428c protein were 12.6% α- helices, 36% β- sheets, 17.5% turn and 33.9% random coil. This data confirmed that the purified protein is in properly folded state.

3.8 Effect of Temperature and pH on Secondary Structure of rRv0428c Protein

The unfolding property of rRv0428c protein was determined by incubating it at temperatures ranging from 30 to 70 °C. The gradual loss of molar ellipticity combined with shift

of minima was used to monitor the state of protein through CD spectroscopic analysis. There was a gradual decrease in negative molar ellipticity of rRv0428c protein with variation in temperature. The Rv0428c protein conformation was stable up to temperatures ≤ 40 °C with subsequent convergence of curves. With increase in temperature beyond 40 °C the protein starting losing its secondary structure (Fig. 4C). The protein exhibited stability over a wide pH range (5.0–9.0), as was evident from gradual change in the negative ellipticity (Fig. 4D).

3.9 Fluorescence Analysis of rRv0428c

To study the effect of temperature on the tertiary structure of Rv0428c protein, intrinsic tryptophan fluorescence spectroscopy was done. The Rv0428c protein has 11 tryptophan amino acid residues. The maximum fluorescence intensity was observed at 340 nm emission wavelength. There was gradual decrease in the intrinsic fluorescence with the subsequent increase in temperature. The peak maxima shifted from 340 to 344 nm by increase in temperature from 60 to 90 °C indicating red shift (Fig. 4E). These results pointed towards the fact that intrinsic fluorescence decreased with subsequent increase in temperature.

3.10 Biochemical Characterization of rRv0428c Protein

As bioinformatics analysis predicted that Rv0428c belongs to GNAT family of histone acetyl transferases (HATs), we proceeded for checking the histone acetyl transferase activity of rRv0428c. rRv0428c was purified to homogeneity and in vitro acetylation assay was performed using bacterially purified H3 histone as substrate. The H3 extracted from eukaryotic AGS cell line was used as positive control (lane 8) because histones from eukaryotic system will have endogenous acetylation. The time dependent in vitro acetylation was also performed. With increase in time a sequential increase in the amount of acetylated histone H3 was observed, proving the acetyltransferases activity of rRv0428c (Fig. 5). The lanes 5–7 demonstrated HAT activity of NC fraction of AGS cell line which was found to be less compared to rRv0428c. Overall, these results signify that rRv0428c protein possessed significant HAT activity, which increased upon subsequent increase in incubation period.

3.11 Colony Morphology and Growth Pattern Analysis of *M. smegmatis* Harbouring *rv0428c*

The colony morphology of *M. smegmatis* harboring *rv0428c* (*Msmeg-pVV16-rv0428c*) and *pVV16* (*Msmeg-pVV16*) cultures were compared. Both the cultures were spread at very low cell density onto M7H10-Kan^{+} plates. A significant

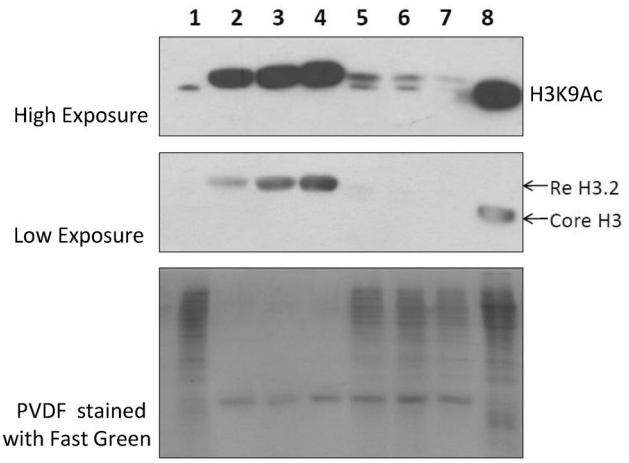

Fig. 5 In vitro acetylation assay for rRv0428c protein, Time dependent acetylation of H3 by rRv0428c, *L1* Nucleocytoplasmic fraction from eukaryotic AGS cell line, *L2* RecH3 + rRv0428c (1 h), *L3* RecH3 + rRv0428c (2 h), *L4* RecH3 + rRv0428c (3 h), *L5* Rec-H3 + AGS NC fraction (1 h), *L6* Rec-H3 + AGS NC fraction (2 h), *L7* Rec-H3 + AGS NC fraction (3 h), *L8* Core histones from AGS cell line

change in the colony morphology of *Msmeg-pVV16-rv0428c* was observed as compared to *Msmeg-pVV16* (Fig. 6A). The *Mmeg-pVV16* colony was rough with a bulge in the centre, whereas, the *Msmeg-pVV16-rv0428c* colony was smooth, wet and flattened.

The growth pattern of *M. smegmatis* containing *rv0428c* was compared with that of the vector *pVV16* alone at different time points- 24 h, 48 h, 72 h and 96 h by CFU counting. Enhanced growth of the *M. smegmatis* harbouring *rv0428c* gene was observed as compared to the *pVV16* vector alone. The *Msmeg-pVV16-rv0428c* in comparison to *Msmeg-pVV16* displayed nearly 1.7 fold enhanced growth after 48 h and 2.8 fold increase in growth after 72 h. The difference in growth was 1.4 fold after 96 h (Fig. 6B).

3.12 Enhanced Survival of *Msmeg-rv0428c* Under Acidic and Nutrient Stress Conditions

For checking the role of *rv0428c* in survival of *M. smegmatis* under acidic conditions in *in-vitro* conditions, both the cultures *Msmeg-pVV16-rv0428c* and *Msmeg-pVV16* were grown in M7H9 media with pH adjusted to 6.0 and 5.0. Then the survival was checked by plating suitable dilutions of the cultures onto M7H10 agar plates having kanamycin at 37 °C. The results showed that the *Msmeg-pVV16-rv0428c* was able to survive under acidic conditions with survival being more significant at pH 6.0 as compared to pH 5.0. *Msmeg-pVV16-rv0428c* culture had a twofold increase in survival in comparison to the recombinant *M. smegmatis* culture harbouring *pVV16* alone at pH 6.0 and 5.0 (Fig. 7A).

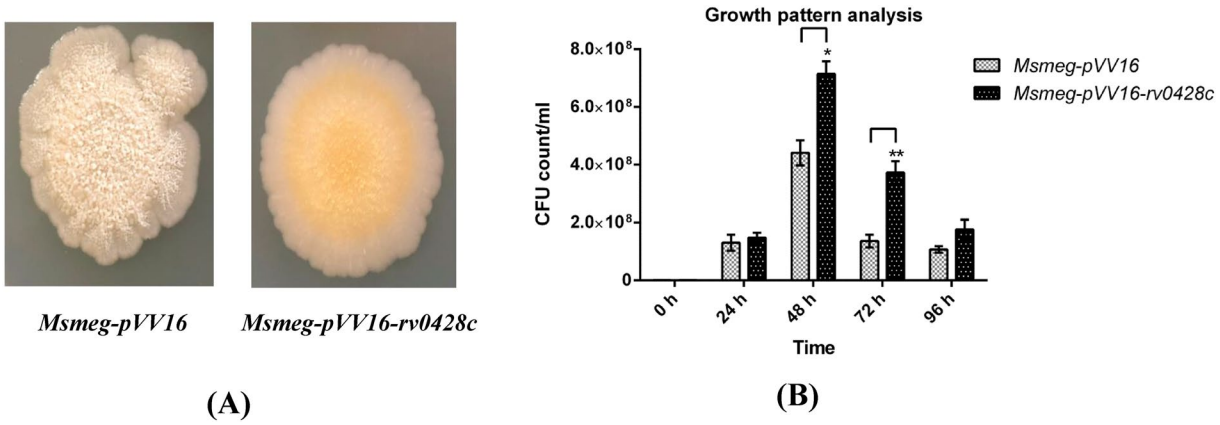

Fig. 6 **A** Effect of *rv0428c* on colony morphology: Enlarged view of single colony of *Msmeg-pVV16* and *Msmeg-pVV16-rv0428c* **B** Growth pattern analysis of *Msmeg-pVV16* and *Msmeg-pVV16-rv0428c* at different time intervals- 24 h, 48 h, 72 h and 96 h Given values are expressed in mean ± *SD* performed in three independent experiments. Statistical analysis was assessed using student's *t*-test (*$p \leq 0.05$ and **$p \leq 0.01$)

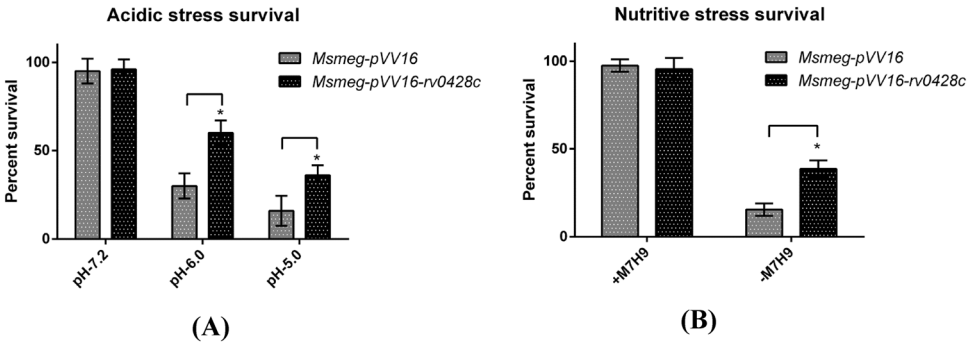

Fig. 7 **A** Survival of *Msmeg-pVV16-rv0428c* in comparison to *Msmeg-pVV16* at pH 6.0 and 5.0 **B** Survival of *Msmeg-pVV16-rv0428c* and *Msmeg-pVV16* under nutritive deprived conditions. Data are representative of three independent biological replicates and shown as mean ± *SD*. Statistical analysis was assessed using student's *t*-test (*$p \leq 0.05$)

Both the recombinant *M. smegmatis* culures were also exposed to nutrient stress conditions by incubating the cultures in 1X PBS instead of the M7H9 growth media. There was a 2.5 fold increase in survival of the test culture in comparison to control in the presence of nutrient deprived conditions (Fig. 7B).

3.13 Susceptibility of *Msmeg-rv0428c* to Chloramphenicol

Drug susceptibility of *Msmeg-pVV16-rv0428c* and *Msmeg-pVV16* cultures was checked using resazurin as the indicator of viability. The widely used anti-TB drugs- streptomycin, chloramphenicol, isoniazid and rifampicin were used for DST. The *Msmeg-pVV16-rv0428c* culture was able to grow in the presence of chloramphenicol with minimum inhibitory concentration (MIC) of 3 µg/ml. This is evident from the colour change from blue to pink in the 48-well plate (Fig. 8A). The CFU/ml were also monitored which depicted enhanced survival of *Msmeg-pVV16-rv0428c* in comparison to the *Msmeg-pVV16* culture upon incubation with increasing concentration of chloramphenicol (Fig. 8B). The plates with isoniazid, streptomycin and rifampicin showed no colour change indicating that the *M. smegmatis* cultures were susceptible to these drugs.

4 Discussion

M. tuberculosis is unique in its ability to survive for prolonged period within the harsh environment inside the host, specifically within the phagosomal compartment of the host macrophages by inhibiting the maturation of phagosome [25, 26]. Out of 11 mycobacterial proteins exclusively identified in phagosome, 3 proteins, Rv0428c, Rv1130 and Rv1191 were annotated as hypothetical proteins [9]. Since the identification of hypothetical proteins by Cole et al. in 1998, attempts were being made to characterize these hypothetical proteins. Rv0428c protein has been predicted as an ideal candidate for playing a protective role in the survival of mycobacteria inside the adverse host cell environment. The adaptive responses of bacterial species to various environmental stress conditions have been shown to be involving alternative sigma factors [27]. The up regulated expression

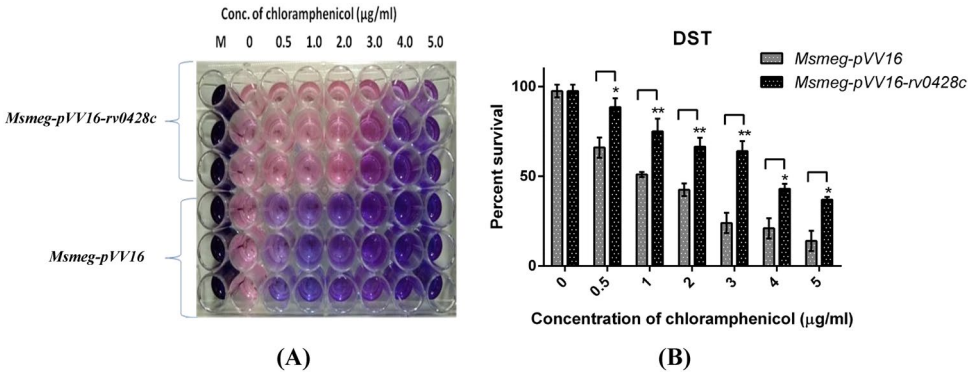

Fig. 8 Plate assay for drug susceptibility testing of chloramphenicol (0.5–10 µg/ml) using resazurin **A** Effect of Rv0428c on drug susceptibility of *Msmeg-pVV16-rv0428c* and *Msmeg-pVV16* cultures**:** Mid log-phase recombinant *M. smegmatis* cultures diluted in 7H9 medium without tween-80 were treated with indicated concentrations of chloramphenicol, with M indicating negative control containing media alone. Resazurin dye in 20% tween 80 was added after 4 h of incubation at 37 °C and the colour change was monitored after 24 h. Pink colour indicates live bacteria, while blue indicates dead bacteria **B** Survival of *Msmeg-pVV16-rv0428c* and *Msmeg-pVV16* was monitored by counting the CFU/mL after treatment with chloramphenicol. Results were expressed in % survival (CFU counts without drug treatment was considered to be the 100% survival). Data are representative of three independent biological replicates and shown as mean ± *SD*. Statistical analysis was assessed using student's *t*-test (*$p \leq 0.05$ and **$p \leq 0.01$)

of *rv0428c* under acidic and nutrient stress conditions and the potential sigma factor binding sites for *sigE* and *sigF* in the nucleotide sequence upstream to the operon suggested their role in the transcriptional regulation under stress conditions. Several mycobacterium genes including *PknG*, *rv3097c* and *rv1169c*, were over expressed under the influence of acidic and nutritive stress, aiding in the survival of *M. tuberculosis* [22, 23, 28].

Rv0428c of *M. tuberculosis* was predicted to be a probable acetyl transferase belonging to the GNAT (GCN5-related acetyl transferase) family of HATs (Histone Acetyl Transferase). ε-amino lysine acetylation was not limited only to histone modification and regulation of transcription, but was reported to be involved in several cellular processes [29]. This might alter the charge on protein, its conformation and protein stability. Acetylomes or genome-wide identification of lysine-acetylated proteins in bacteria has pointed towards wide diversity of functions for lysine acetylated proteins. The GCN5-related N-acetyltransferase (GNAT) super family is a large group of evolutionarily related acetyl transferases, with multiple paralogs in organisms from all kingdoms of life [24, 30]. Although the functional role of protein acetylation in eukaryotes has long been studied, it was recently discovered that acetylation of proteins is common in bacteria as well [31–34]. The GNAT family of transferases have been shown to exhibit sequence homology with a class of eukaryotic transcription factors, the first of which was the yeast GCN5 [35]. As Rv0428c has been predicted to be a member of the GNAT family, we proceeded for docking of Rv0428c with eukaryotic histone H3 tail region and acetyl-co-A to establish the interactions between the substrate histone and donor acetyl-co-A with our protein of interest. The docking analysis predicted multiple hydrogen bonds and hydrophobic interactions between the Rv0428c protein-acetyl-co-A complex and Rv0428c-H3 tail region. Previously, GNAT proteins have been implicated in acetylation of lysine in the core histone H3 tail region [36, 37]. These findings provide substance to the fact that Rv0428c is a probable member of the GNAT family, which might be playing an important role in acetylation of proteins.

The thermal unfolding studies of recombinant Rv0428c using CD spectroscopy revealed that the secondary structure of rRv0428c protein was completely stable up to 40 °C. Previously, multiple tryptophan residues have been implicated in providing stability to the *M. tuberculosis* protein Rv0774c [38]. The Rv0428c protein have 11 tryptophan amino acid residues, however, the conformational changes in the tertiary structure of Rv0428c protein revealed that it was stable up to 60 °C with peak maxima at 340 nm. After 60 °C, red shift is observed leading to shift of peak maxima towards the higher wavelength. An in vitro acetylation assay performed using recombinant histone H3, confirmed the acetyl transferase activity of the protein that increased in time dependent manner. Rv1988, a secretory mycobacterial methyl transferase was localized in the host nucleus and interacted with histone H3 resulting in repression of genes responsible for first line of defence against tuberculosis. The deletion of Rv1988 suppresses the survival of *M. tuberculosis* inside the host [39]. The protein–protein interaction study revealed that Rv0428c showed significant interactions with Rv2416c (eis). Previously, Rv2416c was designated as enhanced intracellular survival (eis), owing to the fact that it was responsible for enhanced survival of *M. smegmatis* inside the macrophage cell line [40].

No homolog of *rv0428c* was found in *M. smegmatis* making it an ideal host candidate for performing in vitro experiments which mimic the mycobacterium species. The over expression of *rv0428c* altered the colony morphology besides increasing the growth rate of *M. smegmatis*. The association of colony morphology with virulence of mycobacterium species is a well established fact. There are previous reports which lend support to the fact that expression of several mycobacterial genes like *rv1169c* [41], *rv1818c* [42] and *rv0774c* [43] altered the colony morphology and growth rate of *M. smegmatis*. The advent of drug-resistant strains of *M. tuberculosis* has led to drug susceptibility testing of individuals complaining of symptoms of tuberculosis. As this makes sure that a particular individual will respond to the prescribed anti-TB drug regimen. The GNATs have been demonstrated to be involved in acetylation of aminoglycoside antibiotics by acting as aminoglycoside modifying enzymes leading to resistance against these antibiotics [44, 45]. revealed that Rv0428c is resistant to chloramphenicol, implicating the role of Rv0428c in conferring drug resistance to Mycobacterium species. The resistance to chloramphenicol could be due to the sequence similarity of Rv0428c with the chloramphenicol acetyl transferase, an enzyme which detoxifies chloramphenicol by acetylation and is responsible for chloramphenicol resistance in bacteria [46]. Further study is required to find out the specific target of this enzyme in *M. tuberculosis* by making the knockout of the gene followed by acetylome analysis.

5 Conclusion

In summary, Rv0428c is the active acetyl transferase belonging to GNAT family of HATs identified in *M. tuberculosis*. It was exclusive to the intraphagosomal compartment of infected macrophages. Rv0428c was stable over a wide range of pH and could retain its tertiary structure upto 60 °C pointing towards its probable role in harsh conditions. It also plays a protective role under nutrient and acidic stress conditions in vitro. The expression of protein resulted in altered colony morphology and enhanced growth of *M. smegmatis* under various stress conditions. The role played by Rv0428c in survival of *M. tuberculosis* under the stress conditions makes it a probable candidate for drug targeting.

Supplementary Information The online version contains supplementary material available at https://doi.org/10.1007/s10930-022-10044-x.

Acknowledgements The authors duly acknowledge Department of Science and Technology (DST) for the financial assistance to Dr Jagdeep Kaur and University Grants Commission (UGC) for providing fellowship to Aashish Sharma.

Author Contributions JK conceived the idea, designed the study and supervised the research work. AS performed most of the experiments and wrote the manuscript. AK performed the Bioinformatics work. Histone acetylation experiments were carried out by MR and RVA under the supervision of SG at ACTREC, Mumbai.

Funding This work was supported by the Department of Science and Technology (DST), India.

Data Availability The datasets generated during and/or analyzed during the current study are available from the corresponding author on reasonable request.

Declarations

Conflict of interest The authors declare that they have no competing interests.

Ethical Approval Not applicable.

Consent to Participate Not applicable.

References

1. WHO (2020) GLOBAL TUBERCULOSIS REPORT 2020
2. Zignol M, Dean AS, Alikhanova N et al (2016) Population-based resistance of Mycobacterium tuberculosis isolates to pyrazinamide and fluoroquinolones: results from a multicountry surveillance project. Lancet Infect Dis 16:1185–1192. https://doi.org/10.1016/S1473-3099(16)30190-6
3. Sundararajan S, Muniyan R (2021) Latent tuberculosis: interaction of virulence factors in Mycobacterium tuberculosis. Mol Biol Rep 1:1–16. https://doi.org/10.1007/S11033-021-06611-7
4. Cole ST, Brosch R, Parkhill J et al (1998) Deciphering the biology of Mycobacterium tuberculosis from the complete genome sequence. Nature 393:537–544. https://doi.org/10.1038/31159
5. Geiman DE, Raghunand TR, Agarwal N, Bishai WR (2006) Differential gene expression in response to exposure to antimycobacterial agents and other stress conditions among seven mycobacterium tuberculosis whiB-like genes. Antimicrob Agents Chemother 50:2836–2841. https://doi.org/10.1128/AAC.00295-06
6. Vozza EG, Mulcahy ME, McLoughlin RM (2021) Making the most of the host; targeting the autophagy pathway facilitates *Staphylococcus aureus* intracellular survival in neutrophils. Front Immunol. https://doi.org/10.3389/FIMMU.2021.667387
7. Ehrt S, Schnappinger D (2009) Mycobacterial survival strategies in the phagosome: defense against host stresses. Cell Microbiol. https://doi.org/10.1111/j.1462-5822.2009.01335.x
8. Voskuil MI, Bartek IL, Visconti K, Schoolnik GK (2011) The response of mycobacterium tuberculosis to reactive oxygen and nitrogen species. Front Microbiol 2:105. https://doi.org/10.3389/fmicb.2011.00105
9. Mattow J, Siejak F, Hagens K et al (2006) Proteins unique to intraphagosomally grown Mycobacterium tuberculosis. Proteomics 6:2485–2494. https://doi.org/10.1002/pmic.200500547
10. Kim KH, An DR, Song J et al (2012) Mycobacterium tuberculosis Eis protein initiates suppression of host immune responses by acetylation of DUSP16/MKP-7. Proc Natl Acad Sci USA 109:7729–7734. https://doi.org/10.1073/pnas.1120251109
11. Sievers F, Higgins DG (2014) Clustal Omega, accurate alignment of very large numbers of sequences. Methods Mol Biol 1079:105–116. https://doi.org/10.1007/978-1-62703-646-7_6

12. Robert X, Gouet P (2014) Deciphering key features in protein structures with the new ENDscript server. Nucleic Acids Res 42:W320–W324. https://doi.org/10.1093/nar/gku316
13. Szklarczyk D, Franceschini A, Wyder S et al (2015) STRING v10: protein-protein interaction networks, integrated over the tree of life. Nucleic Acids Res 43:D447–D452. https://doi.org/10.1093/nar/gku1003
14. Biasini M, Bienert S, Waterhouse A et al (2014) SWISS-MODEL: modelling protein tertiary and quaternary structure using evolutionary information. Nucleic Acids Res 42:W252–W258. https://doi.org/10.1093/nar/gku340
15. DeLano WL (2004) pymol user's guide
16. Dundas J, Ouyang Z, Tseng J et al (2006) CASTp: computed atlas of surface topography of proteins with structural and topographical mapping of functionally annotated residues. Nucleic Acids Res 34:W116–W118. https://doi.org/10.1093/nar/gkl282
17. Zhang Y (2009) I-TASSER: fully automated protein structure prediction in CASP8. Proteins 77(Suppl 9):100–113. https://doi.org/10.1002/prot.22588
18. Morris GM, Huey R, Lindstrom W, Sanner MF, Belew RK, Goodsell DS, Olson AJ (2009) AutoDock4 and AutoDockTools4: automated docking with selective receptor flexibility. J Comput Chem 30:2785–2791
19. Kumar A, Kaur J (2014) Primer based approach for PCR amplification of high GC content gene: mycobacterium gene as a model. Mol Biol Int 2014:937308. https://doi.org/10.1155/2014/937308
20. Kaur J, Kumar A, Kaur J (2017) Strategies for optimization of heterologous protein expression in *E. coli*: roadblocks and reinforcements. Int J Biol Macromol 106:803. https://doi.org/10.1016/j.ijbiomac.2017.08.080
21. Gong Q, Yang X, Cai W et al (2010) Expression and purification of functional epitope of pigment epithelium-derived factor in *E. coli* with inhibiting effect on endothelial cells. Protein J 29:167–173. https://doi.org/10.1007/S10930-010-9236-6
22. Deb C, Daniel J, Sirakova TD et al (2006) A novel lipase belonging to the hormone-sensitive lipase family induced under starvation to utilize stored triacylglycerol in Mycobacterium tuberculosis. J Biol Chem 281:3866–3875. https://doi.org/10.1074/jbc.M505556200
23. Paroha R, Chourasia R, Mondal R, Chaurasiya SK (2018) PknG supports mycobacterial adaptation in acidic environment. Mol Cell Biochem 443:69–80. https://doi.org/10.1007/s11010-017-3211-x
24. Vetting MW, de Carvalho SLP, Yu M et al (2005) Structure and functions of the GNAT superfamily of acetyltransferases. Arch Biochem Biophys 433:212–226. https://doi.org/10.1016/j.abb.2004.09.003
25. Ge P, Lei Z, Yu Y et al (2021) M tuberculosis PknG manipulates host autophagy flux to promote pathogen intracellular survival. Autophagy. https://doi.org/10.1080/15548627202119389 12
26. Rankine-Wilson LI, Shapira T, Emani CS, Av-Gay Y (2021) From infection niche to therapeutic target: the intracellular lifestyle of Mycobacterium tuberculosis. Microbiology 167:001041. https://doi.org/10.1099/MIC.0.001041
27. Cao J, Dang G, Li H et al (2015) Identification and characterization of lipase activity and immunogenicity of lipl from mycobacterium tuberculosis. PLoS ONE 10:e0138151. https://doi.org/10.1371/journal.pone.0138151
28. Betts JC, Lukey PT, Robb LC et al (2002) Evaluation of a nutrient starvation model of Mycobacterium tuberculosis persistence by gene and protein expression profiling. Mol Microbiol 43:717–731
29. Choudhary C, Kumar C, Gnad F et al (2009) Lysine acetylation targets protein complexes and co-regulates major cellular functions. Science (80-) 325:834–840. https://doi.org/10.1126/science.1175371
30. Dyda F, Klein DC, Hickman AB (2000) GCN5-related N-acetyltransferases: a structural overview. Annu Rev Biophys Biomol Struct 29:81–103. https://doi.org/10.1146/annurev.biophys.29.1.81
31. Hu LI, Lima BP, Wolfe AJ (2010) Bacterial protein acetylation: the dawning of a new age. Mol Microbiol 77:15–21. https://doi.org/10.1111/j.1365-2958.2010.07204.x
32. Yu BJ, Kim JA, Moon JH et al (2008) The diversity of lysine-acetylated proteins in *Escherichia coli*. J Microbiol Biotechnol 18:1529–1536
33. Zhang J, Sprung R, Pei J et al (2009) Lysine acetylation is a highly abundant and evolutionarily conserved modification in *Escherichia Coli*. Mol Cell Proteom 8:215–225. https://doi.org/10.1074/mcp.M800187-MCP200
34. Anand C, Santoshi M, Singh PR, Nagaraja V (2021) Rv0802c is an acyltransferase that succinylates and acetylates Mycobacterium tuberculosis nucleoid-associated protein HU. Microbiology 167:001058. https://doi.org/10.1099/MIC.0.001058
35. Berger SL, Piña B, Silverman N et al (1992) Genetic isolation of ADA2: a potential transcriptional adaptor required for function of certain acidic activation domains. Cell 70:251–265. https://doi.org/10.1016/0092-8674(92)90100-Q
36. Howe L, Auston D, Grant P et al (2001) Histone H3 specific acetyltransferases are essential for cell cycle progression. Genes Dev 15:3144–3154. https://doi.org/10.1101/gad.931401
37. Kuo M-H, Brownell JE, Sobel RE et al (1996) Transcription-linked acetylation by Gcn5p of histones H3 and H4 at specific lysines. Nature 383:269–272. https://doi.org/10.1038/383269a0
38. Kumar A, Singh SM, Singh R, Kaur J (2017) Rv0774c, an iron stress inducible, extracellular esterase is involved in immune-suppression associated with altered cytokine and TLR2 expression. Int J Med Microbiol 307:126–138. https://doi.org/10.1016/J.IJMM.2017.01.003
39. Yaseen I, Kaur P, Nandicoori VK, Khosla S (2015) Mycobacteria modulate host epigenetic machinery by Rv1988 methylation of a non-tail arginine of histone H3. Nat Commun 6:8922. https://doi.org/10.1038/ncomms9922
40. Lella RK, Sharma C (2007) Eis (Enhanced Intracellular Survival) protein of *Mycobacterium tuberculosis* disturbs the cross regulation of T-cells. J Biol Chem 282:18671–18675. https://doi.org/10.1074/jbc.C600280200
41. Singh P, Rao RN, Reddy JRC et al (2016) PE11, a PE/PPE family protein of Mycobacterium tuberculosis is involved in cell wall remodeling and virulence. Sci Rep 6:21624. https://doi.org/10.1038/srep21624
42. Delogu G, Pusceddu C, Bua A et al (2004) Rv1818c-encoded PE_PGRS protein of Mycobacterium tuberculosis is surface exposed and influences bacterial cell structure. Mol Microbiol 52:725–733. https://doi.org/10.1111/j.1365-2958.2004.04007.x
43. Kaur J, Kumar A, Kaur J (2018) Strategies for optimization of heterologous protein expression in *E. coli* : roadblocks and reinforcements. Int J Biol Macromol 106:803–822. https://doi.org/10.1016/j.ijbiomac.2017.08.080
44. Llano-Sotelo B, Azucena EF, Kotra LP et al (2002) Aminoglycosides modified by resistance enzymes display diminished binding to the bacterial ribosomal aminoacyl-tRNA site. Chem Biol 9:455–463
45. Zaunbrecher MA, Sikes RD, Metchock B et al (2009) Overexpression of the chromosomally encoded aminoglycoside acetyltransferase eis confers kanamycin resistance in Mycobacterium tuberculosis. Proc Natl Acad Sci 106:20004–20009. https://doi.org/10.1073/pnas.0907925106
46. Gorman CM, Moffat LF, Howard BH (1982) Recombinant genomes which express chloramphenicol acetyltransferase in mammalian cells. Mol Cell Biol 2:1044–1051